Reliability Analysis of Structures by Active Learning Enhanced Sparse Bayesian Regression

Atin Roy, Ph.D.[1]; Subrata Chakraborty, Ph.D., M.ASCE[2]; and Sondipon Adhikari, Ph.D.[3]

Abstract: Adaptive sampling near a limit state is important for metamodeling-based reliability analysis of structures involving an implicit limit state function. Active learning based on the posterior mean and standard deviation provided by a chosen metamodel is widely used for such adaptive sampling. Most studies on active learning-based reliability estimation methods use the Kriging approach, which provides prediction along with its variance. As with the Kriging approach, sparse Bayesian learning-based regression also provides posterior mean and standard deviation. Due to the sparsity involved in learning, it is expected to be computationally faster than the Kriging approach. Motivated by this, active learning-enhanced adaptive sampling-based sparse Bayesian regression is explored in the present study for reliability analysis. In doing so, polynomial basis functions, which do not involve free parameters, are chosen for the sparse Bayesian regression to avoid computationally expensive parameter tuning. The convergence of the proposed approach is attained based on the stabilization of 10 consecutive failure estimates. The effectiveness of the proposed adaptive sparse Bayesian regression approach is illustrated numerically with five examples. **DOI: 10.1061/JENMDT.EMENG-6964.**

Author keywords: Structural reliability; Sparse Bayesian regression; Active learning; Error-based stopping criterion; Adaptive sparse Bayesian regression-Monte Carlo simulation.

Introduction

Reliability analysis of a structure is a theoretical framework to address the effect of uncertainty involved in structural parameters and loads. The main objective of structural reliability analysis (SRA) is to determine the failure probability P_f, which is mathematically defined as

$$P_f = \underset{g(\mathbf{X})<0}{\iiint \cdots \int} f_{\mathbf{X}}(\mathbf{X}) d\mathbf{X} \tag{1}$$

where $\mathbf{X}$ = an n-dimensional vector of involved random variables; $g(\mathbf{X})$ = the limit state function (LSF); and $f_{\mathbf{X}}(\mathbf{X})$ = the joint probability distribution function (PDF). The limit state is defined by $g(\mathbf{X}) = 0$, i.e., the boundary between the safe domain $\{\mathbf{X}|g(\mathbf{X}) > 0\}$ and the failure domain $\{\mathbf{X}|g(\mathbf{X}) < 0\}$. Thus, to obtain the failure probability, one needs to solve the multidimensional integral as defined by Eq. (1), which is a formidable task for real engineering problems. Therefore, several analytical approximations (e.g., first- and second-order reliability methods) and numerical simulation techniques, e.g., Monte Carlo simulation (MCS), importance sampling, and subset simulation were developed (Ditlevsen and Madsen 2005; Haldar and Mahadevan 2000). The MCS technique is the most accurate and conceptually straightforward. However, a large number of simulations is required by the MCS technique to estimate the P_f value with a sufficiently small variance. The uses of variance reduction techniques like importance sampling, subset simulation, etc. are notable in this regard. Such advanced MCS techniques reduce the required number of simulations as usually necessary in the brute-force MCS technique. Still, such techniques require several repetitive evaluations of LSF, particularly for small failure probability, and become computationally demanding for reliability analysis of real engineering problems involving implicit LSF, which requires the solution of high-fidelity numerical models. The metamodeling technique is a powerful means to deal with such situations. Metamodels are trained by a limited number of training samples known as design of experiments (DOE) to substitute the actual LSF with an approximating function. Various metamodeling techniques, e.g., polynomial response surface by least-square method (Faravelli 1989) and moving least-square method (Kim et al. 2005), artificial neural network (Hosni Elhewy et al. 2006; Lagaros et al. 2009), radial basis function (Deng 2006), Kriging metamodel (Kaymaz 2005), polynomial chaos expansion (Blatman and Sudret 2010), support vector machine (SVM) (Li et al. 2006) and support vector regression (SVR) (Ghosh et al. 2018; Roy et al. 2019), relevance vector machine (RVM) (Changcong et al. 2015; Mathur and Samui 2013; Zhou et al. 2013), multivariate adaptive regression splines (Metya et al. 2017), etc. are employed for reliability analysis of problems involving implicit LSF.

The active learning-based adaptive sampling approaches are quite notable for improved estimates of reliability. The approach employs a learning function expressed as a function of the local prediction and its variance obtained from a metamodel. A fully active learning method for SRA was first proposed by Bichon et al. (2008). The method is termed "efficient global reliability analysis," where the expected feasibility function (EFF) is utilized as a learning function. A new training sample is numerically searched by a global optimization from the truncated simulation domain by maximizing the EFF learning function. However, performing the global optimization in each iteration step of the algorithm is expensive to implement. In this regard, the adaptive Kriging combined with the MCS technique (AK-MCS) proposed by Echard et al. (2011) is worth

[1]Dept. of Civil Engineering, Indian Institute of Engineering Science and Technology, Shibpur, Howrah, West Bengal 711103, India. ORCID: https://orcid.org/0000-0002-7353-3903. Email: atin.3222@yahoo.com

[2]Dept. of Civil Engineering, Indian Institute of Engineering Science and Technology, Shibpur, Howrah, West Bengal 711103, India (corresponding author). Email: schak@civil.iiests.ac.in

[3]James Watt School of Engineering, Univ. of Glasgow, Glasgow G12 8QQ, UK. Email: Sondipon.Adhikari@glasgow.ac.uk

Note. This manuscript was submitted on September 14, 2022; approved on January 16, 2023; published online on March 8, 2023. Discussion period open until August 8, 2023; separate discussions must be submitted for individual papers. This paper is part of the ***Journal of Engineering Mechanics***, © ASCE, ISSN 0733-9399.

noting. In the AK-MCS method, a candidate sample set Ω is introduced to represent the entire simulation domain for a quasi-optimum search of the new training sample to update the Kriging model. The sampling concept for active learning in the AK-MCS approach is further modified for rare events, e.g., brute-force MCS is replaced by importance sampling (Echard et al. 2013; Zhang et al. 2020) and by subset simulation (Dubourg et al. 2011; Huang et al. 2016). A recent adaptation of the AK-MCS method for small failure probability (termed AK-MSS) is also notable (Xu et al. 2020). Besides Kriging, other metamodels capable of providing prediction variance were also combined with active learning methods for SRA. Instead of pure Kriging, the polynomial-chaos Kriging approach was coupled with the AK-MCS-based active learning algorithm for SRA (Schöbi et al. 2017). An active learning algorithm that combines sparse polynomial chaos expansions and bootstrap was developed for SRA (Marelli and Sudret 2018). Active learning-based sparse polynomial chaos expansion was also proposed for SRA (Zhou et al. 2020). Cheng and Lu (2021) developed a Bayesian SVR model, which can provide a pointwise probabilistic prediction in active learning algorithms for SRA. Active learning-based adaptive RVM within a probabilistic Bayesian learning framework for SRA was developed by Li et al. (2021).

Similar to the Kriging model, active learning methods can also be readily applied to sparse Bayesian learning-based metamodels. For example, adaptive sampling was employed in the RVM model, a special case of sparse Bayesian learning, for SRA (Changcong et al. 2015; Mathur and Samui 2013; Zhou et al. 2013). However, the implementation of an active learning method for the same is still limited to a recent work by Li et al. (2021). The performances of such RVM models largely depend on the proper selection of the prerequisite Gaussian kernel hyperparameter, which involves a computationally expensive cross-validation method. Thus, sparse Bayesian regressions with other types of basis functions, particularly those that do not involve free parameters, deserve to explore further. Keeping this in view, an active-learning-enhanced adaptive sampling-based sparse Bayesian regression is explored in the present study for SRA. The polynomial basis functions that do not involve free parameters are chosen for the sparse Bayesian regression to avoid computationally expensive hyperparameter tuning. Noting the slow convergence of the stopping criterion proposed by Echard et al. (2011), Wang and Shafieezadeh (2019) proposed an efficient error-based stopping criterion (ESC) for the AK-MCS approach. To study the effectiveness of the ESC, a mathematical test problem is investigated and found unsuitable for the proposed approach. In this regard, the stopping criterion based on the stabilization of 10 consecutive failure estimates is found to be effective in adaptive RVM for SRA (Changcong et al. 2015) and is adopted in the present study. The effectiveness of the proposed approach is demonstrated numerically by considering five examples.

Active Learning Method of Reliability Analysis

The primary task of an active learning method is to optimize a learning function to find the next best training sample. The basic two inputs to most of the active learning functions are the posterior mean and standard deviation (SD) functions. The use of the EFF proposed by Bichon et al. (2008) and the U function proposed by Echard et al. (2011) as learning functions can widely be noted. Between these two, the U function is found to be more suitable for the active learning-based reliability analysis method (Echard et al. 2011). Hence, the U function is employed as the active learning function in the present study. It is defined by Echard et al. (2011)

$$U(\mathbf{x}) = \frac{|\hat{\mu}(\mathbf{x})|}{\hat{\sigma}(\mathbf{x})} \tag{2}$$

where $\hat{\mu}(\mathbf{x})$ and $\hat{\sigma}(\mathbf{x})$ = the posterior mean and SD functions, respectively. The best point is obtained to minimize the U function, i.e., $\min(U(\mathbf{x}))$ for $\mathbf{x} \in \Omega$ (Echard et al. 2011).

Apart from the learning function, proposing a suitable stopping criterion is also an important component of an active learning algorithm for reliability analysis. Noting the limitation of the stopping criteria of the U function and the EFF learning function, the efficient ESC was proposed by Wang and Shafieezadeh (2019). In this criterion, an upper bound for the error $\hat{\varepsilon}_{\max}$ is estimated for a given confidence level by leveraging the statistical information available in the Kriging approach, and an error threshold ε_{thr} is prescribed. The ESC is defined as $\hat{\varepsilon}_{\max} \leq \varepsilon_{thr}$, expecting that the true error ε should be smaller than $\hat{\varepsilon}_{\max}$. The necessary formulae for estimating $\hat{\varepsilon}_{\max}$ is briefly presented here for ready reference; the detailed derivation can be found in Wang and Shafieezadeh (2019).

The true failure and safe domains within Ω are denoted by Ω_f and Ω_s, respectively, and the Kriging-based approximated failure and safe domains are referred to as $\hat{\Omega}_f$ and $\hat{\Omega}_s$, respectively. The $\hat{\varepsilon}_{\max}$ is obtained as follows (Wang and Shafieezadeh 2019)

$$\varepsilon_{\max} = \max\left(\left|\frac{\hat{N}_f}{\hat{N}_f - \hat{S}_f^u} - 1\right|, \left|\frac{\hat{N}_f}{\hat{N}_f + \hat{S}_s^u} - 1\right|\right) \tag{3}$$

where $\hat{N}_f$ = the total number of samples in $\hat{\Omega}_f$; $\hat{S}_f^u$ and $\hat{S}_s^u$ = the upper bounds of the confidence interval of $\hat{S}_f$ and $\hat{S}_s$, respectively, for the confidence level $\alpha = 0.05$; $\hat{S}_f$ = the total number of samples in $\hat{\Omega}_f$ that belong to Ω_s; and $\hat{S}_s$ = the total number of samples in $\hat{\Omega}_s$ that belong to Ω_f. The $\hat{S}_s^u$ and $\hat{S}_f^u$ can be expressed as follows (Wang and Shafieezadeh 2019):

$$\hat{S}_s^u = \mu_{\hat{S}_s} + \Phi^{-1}\left(1 - \frac{\alpha}{2}\right)\sigma_{\hat{S}_s}; \qquad \mu_{\hat{S}_s} = \sum_{i=1}^{\hat{N}_s} p_i^{wse};$$

$$\sigma_{\hat{S}_s} = \sum_{i=1}^{\hat{N}_s}(1 - p_i^{wse})p_i^{wse}; \quad \mathbf{x} \in \hat{S}_s \tag{4}$$

$$\hat{S}_f^u = \Gamma_{\hat{S}_f}^{-1}\left(1 - \frac{\alpha}{2}\right), \quad \mu_{\hat{S}_f} = \sum_{i=1}^{\hat{N}_f} p_i^{wse}; \quad \mathbf{x} \in \hat{S}_f \tag{5}$$

where p_i^{wse} = the probability of wrong sign estimation for $\mathbf{x}_i$ and is defined as (Echard et al. 2011), $p_i^{wse} = \Phi(-|\hat{\mu}(\mathbf{x}_i)/\hat{\sigma}(\mathbf{x}_i)|)$; $\Phi(\cdot)$ and $\Phi^{-1}(\cdot)$ = the cumulative density function (CDF) and the inverse CDF of the standard normal distribution, respectively; and $\Gamma_{\hat{S}_f}^{-1}(\cdot)$ = the inverse CDF of the Poisson distribution with both the mean and variance equal to $\mu_{\hat{S}_f}$.

Active Learning-Enhanced Sparse Bayesian Regression for Reliability Analysis

Sparse Bayesian Regression

A general Bayesian framework is used to obtain sparse solutions to regression and classification tasks utilizing models linear in parameters is introduced by Tipping (2001). The prediction is typically based on some function $y(\mathbf{x})$ defined over the input space. The process of inferring this function or its parameters is learning. A flexible and popular set of candidates $y(\mathbf{x})$ can be expressed as

$$y(\mathbf{x};\mathbf{w}) = \sum_{m=1}^{M} \omega_m \phi_m(\mathbf{x}) \tag{6}$$

where the output is a linearly weighted sum of M basis functions $\phi_m(\mathbf{x})$ (generally nonlinear and fixed) with adjustable parameters or weights, ω_m. The Bayesian probabilistic framework for learning in the general model of the form, as given by Eq. (6), is briefly presented in the following.

Given a training data set $\{\mathbf{x}_i, t_i\}_{i=1}^{P}$, the sparse Bayesian regression model follows the standard probabilistic formulation and assumes that the targets $\mathbf{t} = \{t_1, t_2, \ldots, t_P\}^{\mathrm{T}}$ are samples from the model $\mathbf{y} = \{y(\mathbf{x}_1), y(\mathbf{x}_2), \ldots, y(\mathbf{x}_P)\}^{\mathrm{T}}$ with additive noise $\boldsymbol{\varepsilon} = \{\varepsilon_1, \varepsilon_2, \ldots, \varepsilon_P\}^{\mathrm{T}}$ as

$$\mathbf{t} = \mathbf{y} + \boldsymbol{\varepsilon} = \boldsymbol{\Phi}\mathbf{w} + \boldsymbol{\varepsilon} \tag{7}$$

where $\mathbf{w} = \{\omega_1, \omega_2, \ldots, \omega_M\}^{\mathrm{T}}$ = the parameter vector; and $\boldsymbol{\Phi}$ = a $P \times M$ design matrix whose P rows correspond to P training data, and each row contains M basis functions. The vector $\boldsymbol{\varepsilon}$ consists of independent samples from some noise process assumed to be zero mean Gaussian with variance σ^2, i.e., $p(\boldsymbol{\varepsilon}) = \prod_{i=i}^{P} \mathcal{N}(\varepsilon_i|0,\sigma^2)$. Thus, the error model implies a multivariate Gaussian likelihood of the data set as

$$p(\mathbf{t}|\mathbf{w},\sigma^2) = (2\pi\sigma^2)^{-P/2} \exp\left(-\frac{\|\mathbf{t}-\boldsymbol{\Phi}\mathbf{w}\|^2}{2\sigma^2}\right) \tag{8}$$

It is to be noted here that, for as many parameters in the model as training examples, the maximum likelihood estimation of $\mathbf{w}$ and σ^2 from Eq. (8) would lead to severe overfitting. To circumvent this, the parameters are constrained by defining an explicit prior probability distribution over them. A zero-mean Gaussian prior distribution over $\mathbf{w}$, with a vector of M independent hyperparameters, $\boldsymbol{\alpha} = \{\alpha_1, \alpha_2, \ldots, \alpha_M\}^{\mathrm{T}}$ is formulated as

$$p(\mathbf{w}|\boldsymbol{\alpha}) = \prod_{m=1}^{M} N(\omega_m|0,\alpha_m^{-1}) = (2\pi)^{-M/2} \prod_{m=1}^{M} \alpha_m^{1/2} \exp\left(-\frac{\alpha_m \omega_m^2}{2}\right) \tag{9}$$

The presented formulation of the prior distributions in Eq. (9) is a type of automatic relevance determination prior (Tipping 2001), which is eventually responsible for the sparsity property of the model. In the context of the Bayesian interface, the posterior distribution over the weights can be obtained as follows (Tipping 2001)

$$p(\mathbf{w}|\mathbf{t},\boldsymbol{\alpha},\sigma^2) = \frac{p(\mathbf{t}|\mathbf{w},\sigma^2)p(\mathbf{w}|\boldsymbol{\alpha})}{p(\mathbf{t}|\boldsymbol{\alpha},\sigma^2)} = (2\pi)^{-M/2}|\boldsymbol{\Sigma}|^{-1/2} \exp\left\{-\frac{1}{2}(\mathbf{w}-\boldsymbol{\mu})^T\boldsymbol{\Sigma}^{-1}(\mathbf{w}-\boldsymbol{\mu})\right\} \tag{10}$$

where the posterior covariance $\boldsymbol{\Sigma}$ and the mean $\boldsymbol{\mu}$ are given as

$$\boldsymbol{\Sigma} = (\mathbf{A} + \sigma^{-2}\boldsymbol{\Phi}^{\mathrm{T}}\boldsymbol{\Phi})^{-1} \quad \text{and} \quad \boldsymbol{\mu} = \sigma^{-2}\boldsymbol{\Sigma}\boldsymbol{\Phi}^{\mathrm{T}}\mathbf{t} \tag{11}$$

where A is defined as the diag($\boldsymbol{\alpha}$). Extending the model to include Bayesian inference over the hyperparameters, $\boldsymbol{\alpha}$ is theoretically intractable. Therefore, a most-probable point estimate $\boldsymbol{\alpha}_{MP}$ can be found by a Type-II maximum likelihood procedure (Tipping and Faul 2003). Sparse Bayesian learning is formulated as the (local) maximization of the marginal likelihood or equivalently its logarithm with respect to $\boldsymbol{\alpha}$ as follows:

$$\mathcal{L}(\boldsymbol{\alpha}) = \log p(\mathbf{t}|\boldsymbol{\alpha},\sigma^2) = \log \int_{-\infty}^{\infty} p(\mathbf{t}|\mathbf{w},\sigma^2)p(\mathbf{w}|\boldsymbol{\alpha})d\mathbf{w} = -\frac{1}{2}[P\log 2\pi + \log|\mathbf{C}| + \mathbf{t}^{\mathrm{T}}\mathbf{C}^{-1}\mathbf{t}] \tag{12}$$

where $C = \sigma^2\mathbf{I} + \boldsymbol{\Phi}\mathbf{A}^{-1}\boldsymbol{\Phi}^{\mathrm{T}}$. Finally, after convergence of the hyperparameter estimation procedure, the prediction and its variance at a point of interest $\mathbf{x}_*$ are made by evaluating $\boldsymbol{\Sigma}_{MP}$ and $\boldsymbol{\mu}_{MP}$ from Eq. (11) with $\boldsymbol{\alpha} = \boldsymbol{\alpha}_{MP}$ and $\sigma^2 = \sigma^2_{MP}$ as

$$y_* = \boldsymbol{\phi}(\mathbf{x}_*)\boldsymbol{\mu}_{MP} \tag{13}$$

$$\sigma_*^2 = \sigma_{MP}^2 + \boldsymbol{\phi}(\mathbf{x}_*)\boldsymbol{\Sigma}_{MP}\boldsymbol{\phi}(\mathbf{x}_*)^{\mathrm{T}} \tag{14}$$

where $\boldsymbol{\phi}(\mathbf{x}_*)$ = a row vector containing M elements corresponding to the values of M basis functions at $\mathbf{x}_*$. The implementation of the sparse Bayesian regression presented above can be performed in the MATLAB platform using the SparseBayes 2.0 code available at http://www.relevancevector.com.

Study on Stopping Criterion of Active Learning Algorithm with Sparse Bayesian Regression

A mathematical test problem is taken up for a case study to explore a suitable stopping criterion for the present active learning-based sparse Bayesian regression algorithm. In doing so, the sparse Bayesian regression is employed in the active learning algorithm with the U function as the learning function to study its efficiency in reliability analysis. Two potential stopping criteria are studied. The stopping criterion employed for the adaptive RVM for SRA (Changcong et al. 2015) is considered first where the convergence is considered to attain if 10 consecutive failure estimates are within a negligible discrepancy (e.g., <1%) from each other. In addition, the ESC approach (Wang and Shafieezadeh 2019) is also considered. To study the performance of these two criteria, no stopping criterion is applied in the reliability estimation; rather, learning is allowed up to a large training size (about 350, a moderately high value). The maximum percentage deviation observed among the failure estimates of the preceding 10 iterations and the values of estimated maximum error $\hat{\varepsilon}_{\max}$ (a convergence parameter checked in case of ESC stopping criterion) at each iteration step are calculated.

The test problem is a mathematical function where the number of variables can be changed to study the performance for different input dimensions. The LSF is given as

$$g(\mathbf{X}) = Y_{\text{allow}} - \sum_{i=1}^{n} x_i^2 - \left(\sum_{i=1}^{n}\left(\frac{1}{2}\right)ix_i\right)^2 - \left(\sum_{i=1}^{n}\left(\frac{1}{2}\right)ix_i\right)^4, \quad i = 1,2\ldots,n \tag{15}$$

where Y_{allow} = the allowable maximum value of the mathematical function, and all n random inputs are assumed to be lognormal with mean = 10.0 and SD = 1.0. The physical boundary is considered as the mean $\pm$ 3 $\times$ SD for each random variable. Three different values of n (3, 30, and 150) are considered, which can be treated as low, medium, and high dimension problems, respectively. The value of Y_{allow} is taken as 1.5×10^6, 3.6×10^{13}, and 1.12×10^{19} for n = 3, 30, and 150, respectively.

There is no limit to the total number of basis functions that can be considered in sparse Bayesian learning. It can find only the relevant basis functions. The number of relevant terms never exceeds the number of training data used. Basis functions can be broadly categorized into two types, namely, fixed and data-centered. The fixed basis can be linear, nonlinear, or higher-order polynomials.

Sparse Bayesian learning with a data-centered basis function can be referred to as RVM. A Gaussian kernel function (frequently used in SVM or SVR) can be used as a data-centered basis function. However, there is no restriction on employing a basis, which is a concatenation of fixed basis and data-centered basis to implement sparse Bayesian learning using the SparseBayes 2.0 code in the MATLAB platform. Concatenation of linear basis terms and Gaussian kernel functions would be a practical example for such cases. However, the data-centered basis functions are generally made of kernel functions, which may involve prerequisite kernel parameter(s). The proper selection of such parameter(s) has a large influence on the performance of the metamodel. Thus, the uses of such basis functions need to apply a cross-validation method to obtain the involved parameter(s). This results in data wastage and involves additional computational time (Tipping 2001), whereas a fixed basis is free from such disadvantages. Two fixed-type basis, namely, the first- and second-order polynomial functions, are considered here to demonstrate the active learning-enhanced sparse Bayesian regression for reliability estimate.

First-Order Polynomial Basis

The first-order polynomial function can be expressed for n number of variables, $\boldsymbol{\phi}(\mathbf{x}) = [1, x_1, \ldots, x_n]$. A total $(n+1)$ number of basis functions are present in the linear basis. However, the available training data could be less than $(n+1)$. However, this is not a problem in the sparse Bayesian learning approach, as it is capable of finding the relevant terms and their corresponding weights for regression. Thus, a sparse solution to linear regression with probabilistic prediction is obtained by the sparse Bayesian regression approach.

The actual values of $\hat{S}_s$ and $\hat{S}_f$, $\hat{S}_s^u$ and $\hat{S}_f^u$, as defined in the section "Active Learning Method of Reliability Analysis," at each iteration step are plotted in Fig. 1 and labeled as "Actual Ss," "Actual Sf," "UB_Ss," and "UB_Sf," respectively. The values of $\hat{\varepsilon}_{\max}$ and ε, as defined in the section "Active Learning Method of Reliability Analysis," and the maximum percentage deviation observed among the failure estimates of the previous 10 iterations labeled as "Max error," "Actual error," and "Maxdev10," respectively, are also shown in Fig. 1. It is observed that the actual values of $\hat{S}_s$ and $\hat{S}_f$ are drastically reduced after a certain number of iterations, which increase with the dimension of the problem. Up to this certain number of iterations, it is observed that the actual values of $\hat{S}_s$ and $\hat{S}_f$ exceed the upper bounds $\hat{S}_s^u$ and $\hat{S}_f^u$. In such cases, there is a high chance that the max error estimate (i.e., $\hat{\varepsilon}_{\max}$) will be less than the true error (ε), as $\hat{\varepsilon}_{\max}$ depends on the values of $\hat{S}_s^u$ and $\hat{S}_f^u$. This possibility is witnessed in the right-hand side plots of Fig. 1. It is observed that the actual error is higher than the max error. This indicates that the ESC is not a suitable stopping criterion for the proposed active learning algorithm if applied before a certain number of iterations. However, this number is not known beforehand, whereas the actual error is observed to be close to the Maxdev10 in most of the cases.

Second-Order Polynomial Basis

As with the linear basis, a sparse solution to the second-order polynomial regression with probabilistic prediction can also be obtained by sparse Bayesian regression. The second-order polynomial basis can be expressed for n number of variables, $\boldsymbol{\phi}(\mathbf{x}) = [1, x_1, \ldots, x_n, x_1^2, x_1x_2, \ldots, x_{n-1}x_n, x_n^2]$. In Fig. 2, the values of Actual Ss, Actual Sf, UB_Ss, and UB_Sf at each iteration step are shown on the left-hand side of the plot. The values of max error, actual error, and Maxdev10 at each iteration step are shown on the right-hand side for three different dimensions of the test problem. It is observed that the values of Actual Ss or Actual Sf are higher than those of UB_Ss or UB_Sf at the first few iterations for the three-dimensional case but up to a large number of iterations for 30-dimensional and 150-dimensional cases. Accordingly, the actual error values are also observed to be higher than the max error values for all such iterations. Though this observation is similar to the previous case (linear basis); the number of such iterations in the present case is higher than those of the previous for all three dimensions of the problem. Thus, the ESC is found unsuitable for active learning enhanced sparse Bayesian regression using both the first- and second-order polynomial basis functions. On the other hand, the values of Maxdev10 are observed to be close to the actual error (mostly conservative) at each iteration step for all three different dimensions of the problem. This observation is true for both types of polynomial basis functions. Hence, the learning is stopped in the proposed active learning-enhanced sparse Bayesian regression when 10 consecutive failure estimates are within a negligible discrepancy (e.g., <1%) from each other.

Outline of the Proposed Active Learning-Enhanced Sparse Bayesian Regression Algorithm

Based on the observations in the existing literature on the studies of active learning-based reliability analysis approaches and the case study of the mathematical test problem presented in the previous section, an active learning method is proposed for adaptive sparse Bayesian regression-based reliability analysis. The adaptive sampling strategy of the active learning part remains similar to the AK-MCS method (Echard et al. 2011), as it makes the optimization of the learning function simple yet effective. The posterior mean and SD functions in Eq. (2) are obtained by the sparse Bayesian regression approach instead of the Kriging approach. The proposed active learning-enhanced sparse Bayesian regression is referred to as ASBR-MCS.

In detail, a Monte Carlo population (Ω) within the input space is generated first to start the proposed ASBR-MCS algorithm. Then, 12 samples are randomly selected from this population to build an initial DOE. The iterative enrichment of the DOE with adaptive sampling to improve the failure estimate is performed based on active learning. As mentioned, the U function is taken as the learning function in the present study. However, to obtain the value of the U function at all the points in Ω, the posterior mean and SD are obtained by the sparse Bayesian regression. The point corresponding to the maximum value of the U function is added to the DOE. Specifically, based on the observations of the case study in the previous section, the stopping criterion is adopted judiciously. The philosophy is to know if the accuracy of a learner has reached a plateau, and acquiring more data is likely a waste of resources. The learning of the proposed algorithm is stopped when 10 consecutive iterations provide the failure estimates within a negligible discrepancy from each other. In the proposed algorithm, the negligible discrepancy is considered as 1%. Thus, the considered stopping criterion for learning restricts unnecessary wastage of data. Now, after stopping the learning, the proposed ASBR-MCS algorithm is terminated if the coefficient of variation (COV) of P_f is less than 5%. Otherwise, the population Ω is updated, and the P_f value is estimated again to check the stopping condition. The learning is continued until the stopping condition is satisfied. The steps of the proposed ASBR-MCS approach are summarized in the following (a flowchart is presented in Fig. 3).

1. Generate a Monte Carlo population Ω of size N_{MC} by random sampling in the design space;
2. Select an initial DOE (12 points are randomly selected from Ω);
3. Compute the model parameters for the sparse Bayesian regression according to the DOE;

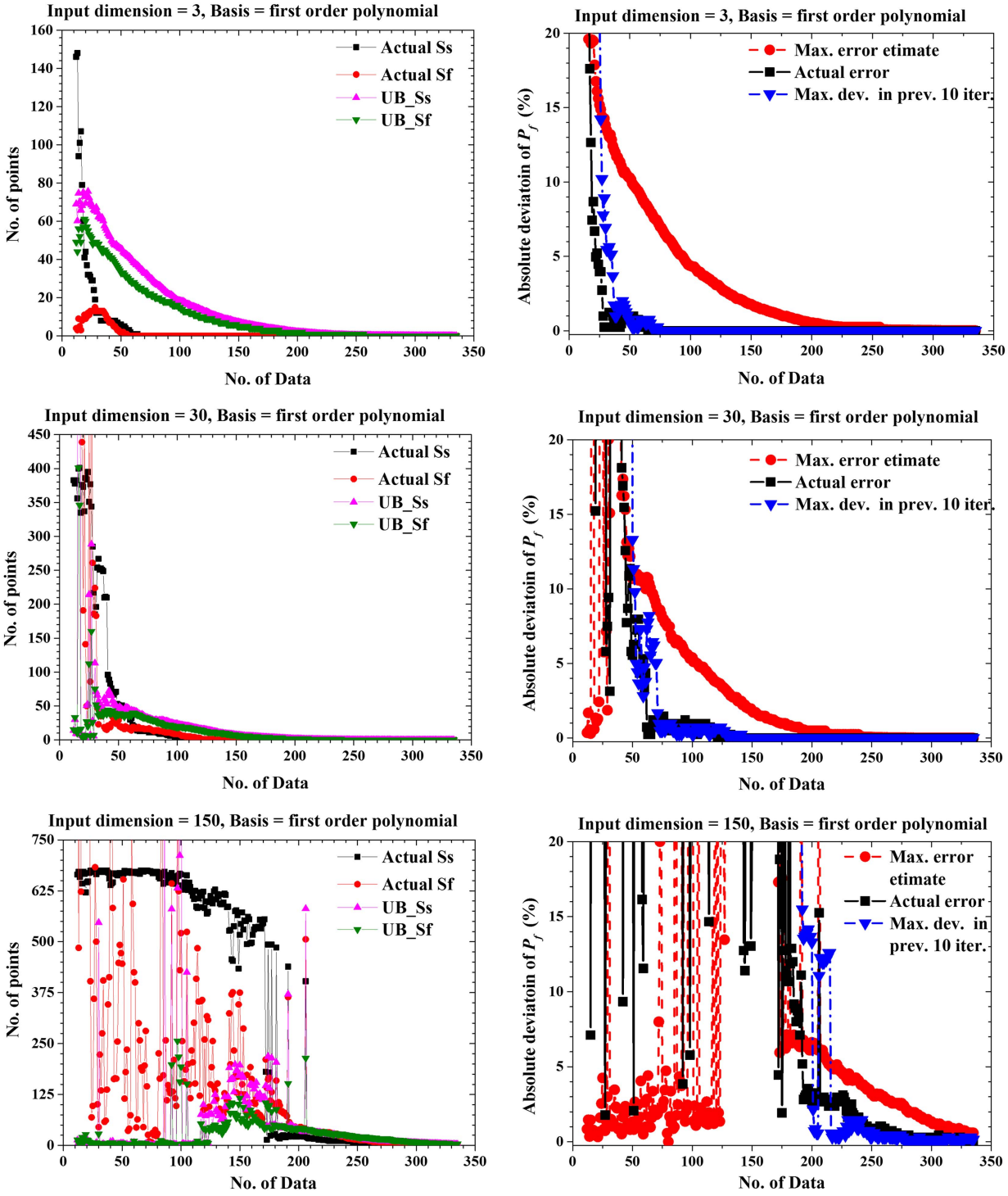

Fig. 1. Active learning-enhanced sparse Bayesian regression with first-order polynomial basis.

4. Compute the LSF prediction and its variance at all the points in the Ω by the sparse Bayesian regression model;
5. Estimate the P_f value and its COV;
6. Check the stopping condition on learning after the first 10 iterations (the maximum deviation among the P_f values of the last 10 iterations should be within 1%); if satisfied, go to Step 9;
7. Calculate the U function at all the points in Ω for identification of the next best point;
8. Update the DOE with the next best point and go to Step 3; and
9. Update the population if the coefficient of variation is higher than 5% and go to Step 4 else stop.

Numerical Study

The effectiveness of the proposed ASBR-MCS approach for reliability analysis is elucidated by considering five example problems. In doing so, the first- and second-order polynomial basis functions are considered. The two ASBR-MCS approaches are referred to as ASBR-P1-MCS and ASBR-P2-MCS for the first- and second-order polynomial basis functions, respectively. The reference results are obtained by the brute-force MCS technique using the actual LSF. The results are also compared with the ESC-enhanced AK-MCS method (Wang and Shafieezadeh 2019). The AK-MCS method uses

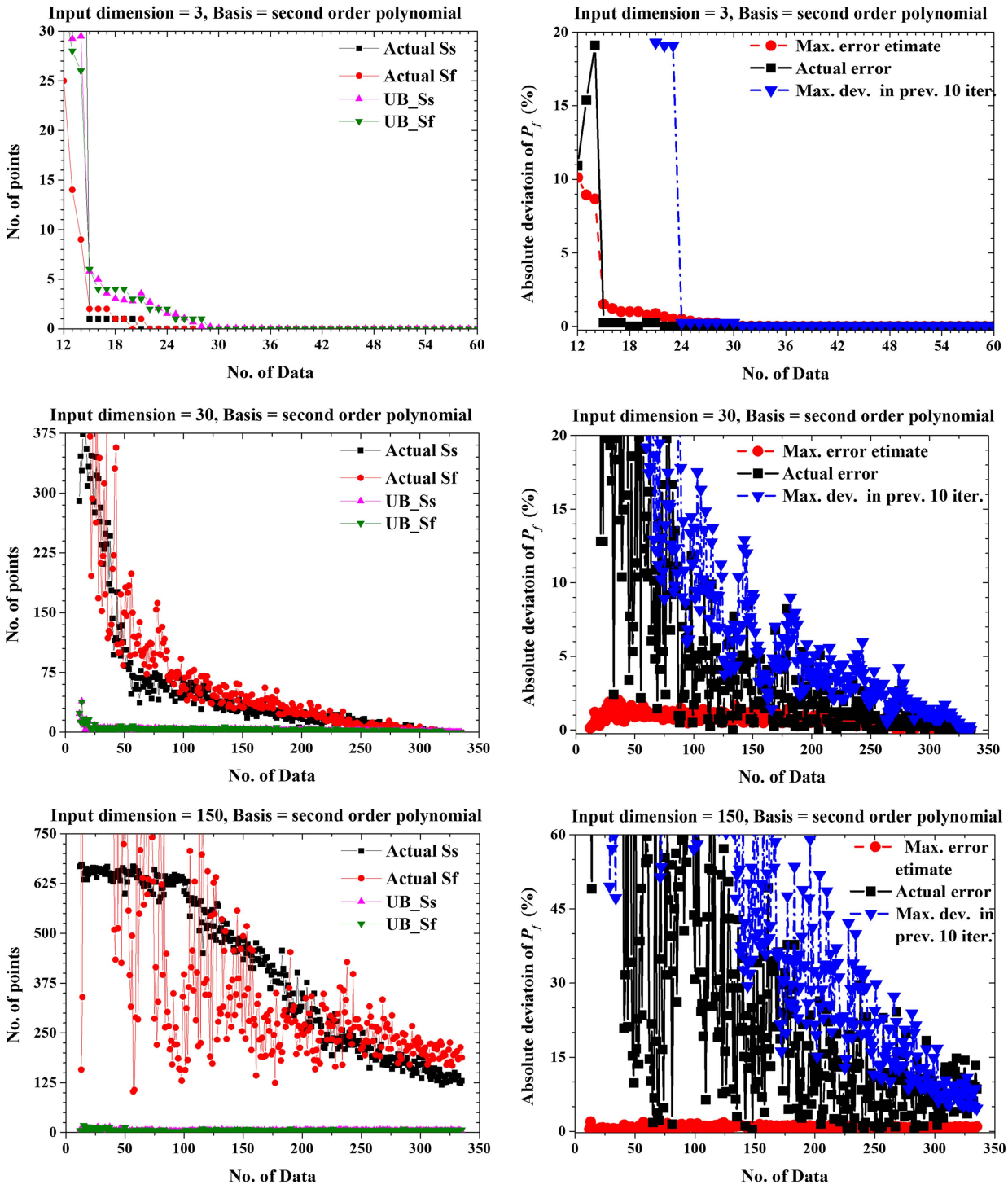

Fig. 2. Active learning-enhanced sparse Bayesian regression with second-order polynomial basis.

the ordinary Kriging method (the regression part contains only a constant). The AK-MCS approach is referred to as AK-P0-MCS.

Example 1: 10-Bar Truss Problem

A 10-bar truss, as shown in Fig. 4, is taken as the first example to demonstrate the effectiveness of the proposed algorithm. Six different structural parameters are considered random. The distribution of each random variable is truncated by the corresponding physical bound, which is taken as mean $\pm$ 3 $\times$ SD of the respective variable. The cross-section areas of the horizontal (A_1), vertical (A_2), and diagonal (A_3) members are assumed to be normal random with mean values of 7.5×10^{-3} m^2, 1.5×10^{-3} m^2, and 5.0×10^{-3} m^2, respectively. Young's modulus (E) of the truss members is also assumed to be normal with a mean value of 70 GPa. The length (L) and load (P) follow a lognormal and a Gumbel max distribution, respectively. The mean values of L and P are considered as 9.0 m and 350.0 kN, respectively. The COV of the cross-section areas and load P are taken as 0.1 and that of E and L are taken as 0.05. The LSF for reliability analysis is considered as follows:

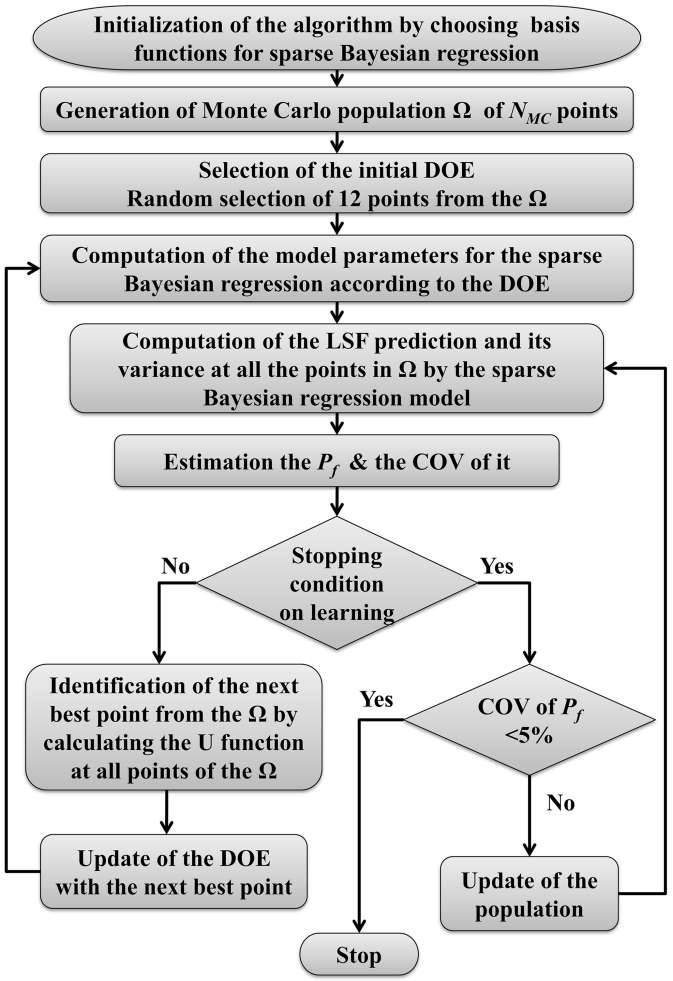

Fig. 3. Flowchart of the proposed ASBR-MCS method.

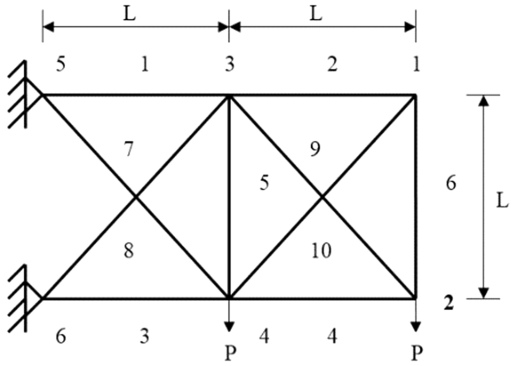

Fig. 4. The planar 10-bar truss. (Reprinted with permission from Springer Nature: Springer, *Reliability-based Structural Design*, "Methods of Structural Reliability," S.-K. Choi, R. V. Grandhi, and R. A. Canfield, © 2007.)

$$g = d_{\text{allow}} - d \tag{16}$$

where d and d_{allow} are the actual displacement under the considered load and the allowable displacement of Node 2. The displacement of Node 2 is obtained using the following explicit relation as provided in Choi et al. (2007)

$$d = \frac{PL}{A_1 A_3 E D_T}\left[4\sqrt{2}A_1^3(24A_2^2 + A_3^2) + A_3^3(7A_1^2 + 26A_2^2) + 4A_1A_2A_3 \times \left\{(20A_1^2 + 76A_1A_2 + 10A_3^2) + \sqrt{2}A_3(25A_1 + 29A_2)\right\}\right] \tag{17}$$

where $D_T = 4A_2^2(8A_1^2 + A_3^2) + 4\sqrt{2}A_1A_2A_3(3A_1 + 4A_2) + A_1A_3^2(A_1 + 6A_2)$. However, for illustration of the present algorithm, the displacement d is approximated by the metamodels.

The failure probabilities for different d_{allow} values are obtained by the ASBR-P1-MCS and ASBR-P2-MCS approaches. A population of 10^5 samples are taken for the brute-force MCS, and the reference results are obtained using the actual LSF defined by Eq. (17). For smaller failure probability cases (i.e., $d_{\text{allow}} = 0.12$ m and 0.125 m), the MCS sample size is increased to 4×10^5. The P_f values are also obtained by the ESC-based AK-P0-MCS method with two different error thresholds, ε_{thr}, i.e., 5% and 1%. The reference results and the errors in the estimated P_f values by different active learning methods, as well as the number of actual function evaluations, are presented in Table 1. The absolute error in estimating the P_f value is calculated as $|1 - \hat{P}_f/P_f| \times 100\%$, where P_f and $\hat{P}_f$ are the probability of failure obtained by the brute-force MCS technique and the considered metamodel. The confidence interval of the failure probability corresponds to a 95% confidence level, which is estimated from the posterior distribution of the corresponding metamodel using Eqs. (4) and (5). The lower and upper bounds of the confidence interval are defined as $(\hat{N}_f - \hat{S}_f^u)/N_{MC}$ and $(\hat{N}_f + \hat{S}_s^u)/N_{MC}$, respectively. The absolute error, the number of training data required, and the lower and upper bounds of the confidence interval are also shown in Table 1. It is observed that the proposed ASBR-P1-MCS approach takes more training data (seen in the case study also) and is less accurate than the ASBR-P2-MCS approach. This is attributed to the presence of nonlinear terms in the second-order polynomial. This gives an advantage to the ASBR-P2-MCS approach for better approximation of LSF over the ASBR-P1-MCS approach, where only linear terms are used as basis functions. The proposed ASBR-P2-MCS approach estimates the P_f values quite accurately (less than 1% error) for all the values of d_{allow} considered. The errors in estimating the P_f values by the ESC-based AK-P0-MCS method with $\varepsilon_{thr} = 5\%$ and 1% are observed to be below 5% and 1%, respectively. The accuracy of the proposed ASBR-P2-MCS approach and the ESC-based AK-P0-MCS approach for $\varepsilon_{thr} = 1\%$ are comparable (errors are less than 1% in both cases). However, the present approach takes fewer iterations and training data. Hence, the proposed ASBR-P2-MCS approach is found to be more efficient than the ESC-based AK-P0-MCS method. The P_f values at each iteration for various active learning methods are shown in Fig. 5. The performances of various approaches at each iteration step with identical learning functions can be readily observed from the figure. It is seen that the active learning function improves the estimate of all three approaches (AK-P0-MCS, ASBR-P1-MCS, and ASBR-P2-MCS). However, the level of improvement is different from one approach to another.

Example 2: Space-Dome Truss Problem

The second problem deals with the reliability analysis of a space-dome truss (as shown in Fig. 6). The LSF is considered with respect to the maximum vertical displacement of the node where the load P_1 is acting. The implicit LSF can be expressed as (Keshtegar 2017)

$$g = \Delta_{\text{allow}} - |\Delta_{P_1}^z| \tag{18}$$

Table 1. Results of different reliability methods for the 10-bar truss

Reliability method	Stopping criteria	P_f for d_{allow} = 0.1 m	0.105 m	0.11 m	0.115 m	0.12 m	0.125 m
MCS	—	6.469×10^{-2}	3.195×10^{-2}	1.493×10^{-2}	6.51×10^{-3}	2.498×10^{-3}	8.96×10^{-4}
		P_f, absolute error, number of data [lower and upper bounds of confidence interval]					
AK-P0-MCS	ESC, $\varepsilon_{thr} = 5\%$	6.263×10^{-2}, 3.18%, 12 + 9 [5.993×10^{-2}, 6.578×10^{-2}]	3.174×10^{-2}, 0.66%, 12 + 12 [3.053×10^{-2}, 3.293×10^{-2}]	1.465×10^{-2}, 1.88%, 12 + 15 [14.01×10^{-2}, 1.533×10^{-2}]	6.67×10^{-3}, 2.46%, 12 + 18 [6.4×10^{-3}, 6.947×10^{-3}]	2.52×10^{-3}, 0.88%, 12 + 18 [2.42×10^{-3}, 2.624×10^{-3}]	9.12×10^{-4}, 1.79%, 12 + 18 [8.72×10^{-4}, 9.44×10^{-4}]
	ESC, $\varepsilon_{thr} = 1\%$	6.487×10^{-2}, 0.28%, 12 + 30 [6.43×10^{-2}, 6.545×10^{-2}]	3.2×10^{-2}, 0.16%, 12 + 28 [3.169×10^{-2}, 3.226×10^{-2}]	1.49×10^{-2}, 0.20%, 12 + 39 [1.476×10^{-2}, 1.502×10^{-2}]	6.51×10^{-3}, 0.00%, 12 + 38 [6.45×10^{-3}, 6.561×10^{-3}]	2.504×10^{-3}, 0.24%, 12 + 44 [2.482×10^{-3}, 2.528×10^{-3}]	8.98×10^{-4}, 0.22%, 12 + 34 [8.9×10^{-4}, 9.06×10^{-4}]
ASBR-P1-MCS	Maxdev10 < 1%	6.362×10^{-2}, 1.65%, 12 + 43 [5.918×10^{-2}, 6.884×10^{-2}]	3.067×10^{-2}, 4.01%, 12 + 43 [3.077×10^{-2}, 3.339×10^{-2}]	1.439×10^{-2}, 3.62%, 12 + 47 [1.277×10^{-2}, 1.660×10^{-2}]	5.65×10^{-3}, 13.21%, 12 + 27 [4.86×10^{-3}, 6.80×10^{-3}]	2.312×10^{-3}, 7.45%, 12 + 48 [1.99×10^{-3}, 2.772×10^{-3}]	8.52×10^{-4}, 4.91%, 12 + 41 [6.96×10^{-4}, 11.23×10^{-4}]
ASBR-P2-MCS	Maxdev10 < 1%	6.481×10^{-2}, 0.19%, 12 + 24 [6.422×10^{-2}, 6.504×10^{-2}]	3.181×10^{-2}, 0.44%, 12 + 25 [3.155×10^{-2}, 3.207×10^{-2}]	1.492×10^{-2}, 0.07%, 12 + 31 [1.471×10^{-2}, 1.520×10^{-2}]	6.46×10^{-3}, 0.77%, 12 + 27 [6.37×10^{-3}, 6.51×10^{-3}]	2.498×10^{-3}, 0.00%, 12 + 42 [2.456×10^{-3}, 2.543×10^{-3}]	8.86×10^{-4}, 1.12%, 12 + 32 [8.78×10^{-4}, 9.00×10^{-4}]

where $\Delta^z_{P_1}$ = the maximum vertical displacement of the node under the load P_1, and Δ_{allow} is its maximum allowable value. The maximum displacement $\Delta^z_{P_1}$ is obtained by using the finite element (FE) analysis software ANSYS. A total of six independent random variables are considered. The distribution of each random variable is truncated by the corresponding physical bound. The bound is taken as mean ± 30% of the mean value of the corresponding random variable. Young's modulus (E) of all members and cross-section areas of top radial bars (A_1 for bar numbers 1–6), peripheral bars (A_2 for bar numbers 7–12), and bottom inclined bars (A_3 for bar numbers 13–24) are assumed as normal random variables. The COVs of A_1, A_2, and A_3 are taken as 0.1 and that of E is 0.05. The point loads P_1 and P_2 (as shown in Fig. 6) follow Gumbel max distributions with mean values of 20 and 10 kN, respectively. The COVs of P_1 and P_2 are taken as 0.15 and 0.12, respectively.

The P_f values for four different values of Δ_{allow} are estimated by the proposed ASBR-P1-MCS and ASBR-P2-MCS approaches. In this problem, 10^5 Monte Carlo samples are considered. The results are also obtained by the ESC-based AK-P0-MCS approach for $\varepsilon_{thr} = 5\%$ and 1%. The reference results and the errors in the estimated P_f values by different active learning approaches are presented in Table 2. The number of training data required and the lower and upper bounds of the failure probabilities estimated by the active learning methods are also shown in the same table. Similar to the previous example, it is observed that the ASBR-P1-MCS approach takes more training data than the ASBR-P2-MCS approach. For all four different values of Δ_{allow}, errors for the ASBR-P2-MCS approach are either close to 1% or less than 1%. However, the errors for the ASBR-P1-MCS approach are observed to be higher than 3% in two cases. In most of the cases of the ESC-based AK-P0-MCS method, the true errors are observed to be less than 5% and 1% for $\varepsilon_{thr} = 5\%$ and 1%, respectively. Similar to the previous example, the accuracy of the proposed ASBR-P2-MCS approach is noted to be quite high and comparable with that achieved by the ESC-based AK-MCS method for $\varepsilon_{thr} = 1\%$. However, the proposed ASBR-P2-MCS approach achieves this accuracy with a fewer number of training samples compared with the ESC-based AK-MCS method for this example as well. To observe the improvement in failure estimate through active learning, the P_f values at each iteration step for various active learning methods are shown in Fig. 7. As with the previous example, it is observed that the nature of improvement of estimated P_f values by all three approaches (AK-P0-MCS, ASBR-P1-MCS, and ASBR-P2-MCS) are different.

Example 3: Transient Heat Conduction Problem

A transient heat conduction problem previously studied by Roy and Chakraborty (2020) is chosen to demonstrate the effectiveness of the present metamodeling approach. The task here is to obtain the function $u(t, x, \omega)$ satisfying the partial differential equation as defined below

$$\frac{\partial}{\partial t}(u(t,x,\omega)) = \frac{\partial}{\partial x}\left(\alpha(x,\omega)\frac{\partial}{\partial x}(u(t,x,\omega))\right) + 1,$$
$$x \in [-1,1], t \in [0,T], \omega \in \Omega$$
$$\text{boundary conditions: } u(t,-1,\omega) = u(t,1,\omega) = 0 \text{ and}$$
$$\text{initial condition: } u(0,x,\omega) = 0 \tag{19}$$

where x = the spatial dimension; ω = the dependence on the random conductivity parameter; $\alpha(x, \omega)$ = the spatially varying random field representing the conductivity parameter; and Ω = the sample space of ω. The random field α is characterized by its mean value $\bar{\alpha} = 10$ and covariance function $C_\alpha(x_1, x_2) = \exp(-|x_1 - x_2|)$, $x_1, x_2 \in [-1, 1]$. Using a truncated Karhunen–Loeve expansion considering up to N number of terms, α can be represented as follows:

$$\alpha(x,\omega) = \bar{\alpha} + \sum_{k=1}^{N} \sqrt{\lambda_k}\,\xi_k \phi_k \tag{20}$$

where λ_k and ϕ_k = the kth eigenvalue and corresponding eigenvector of the covariance matrix, respectively; and ξ_k = the kth uncorrelated random variable. The eigenpairs (λ_k and ϕ_k) need to be obtained approximately. In the present study, $\boldsymbol{\xi} \equiv (\xi_1, \xi_2, \ldots, \xi_N)^T$ is assumed to be independent uniform random over the interval [−1, 1]. Further details of the problem with MATLAB scripts to solve this heat equation problem are available at https://web.stanford.edu/~paulcon/projects/SGS_primer. A vector of u values at each spatial grid point at time T can be extracted as the output for

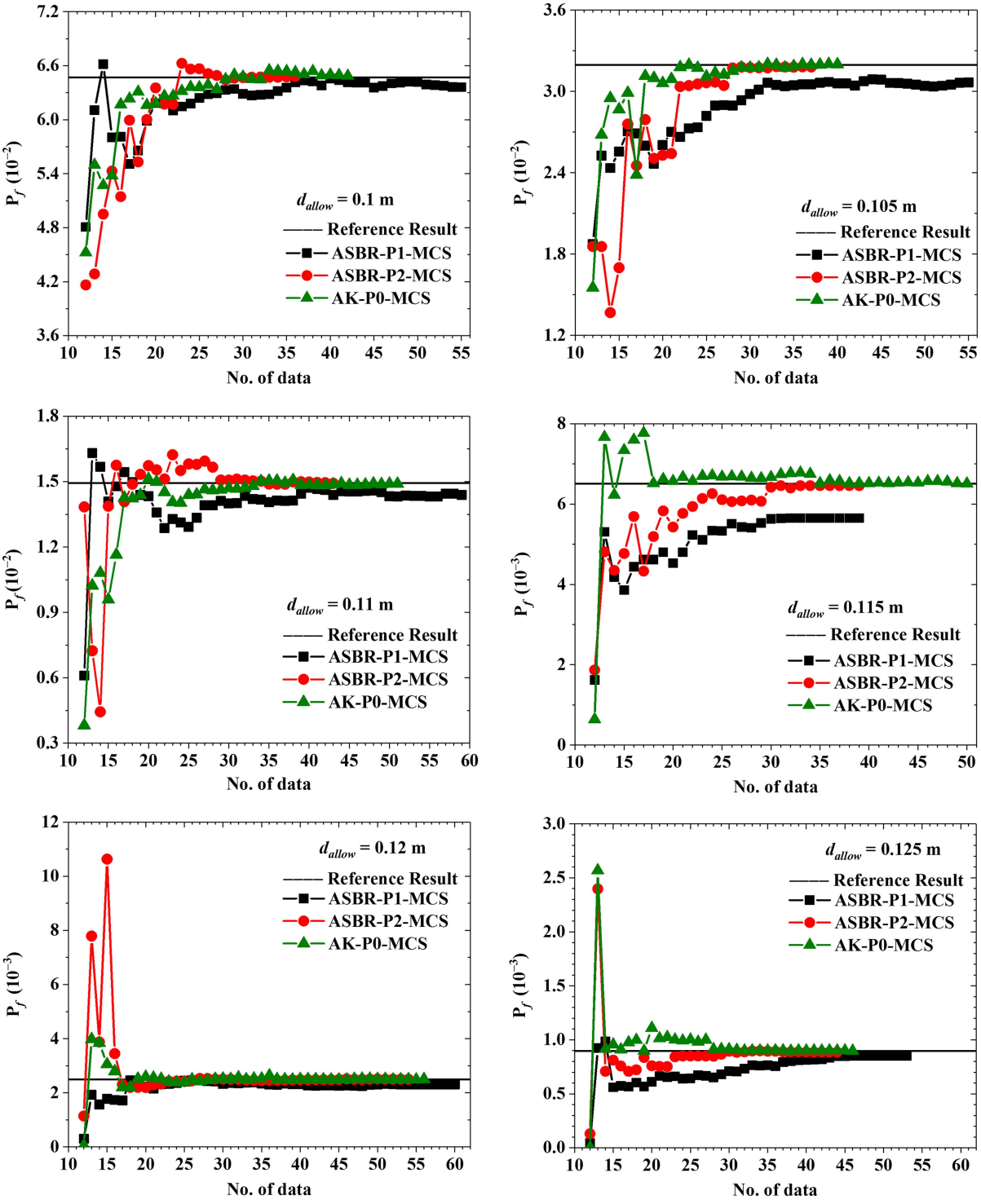

Fig. 5. Comparison of results obtained by different active learning reliability methods for the 10-bar truss.

a certain input value of $\boldsymbol{\xi}$. Thus, the maximum value of u (i.e., $u_{\max}$) is a function of $\boldsymbol{\xi}$ only. The LSF for reliability estimate is considered as follows:

$$g = u_0 - u_{\max} \tag{21}$$

where u_0 is taken as the threshold for $u_{\max}$.

The P_f values for $u_0 = 0.056$ and $N = 75$ are estimated by the proposed ASBR-MCS method and the ESC-based AK-MCS method. A Monte Carlo population of 10^5 samples is considered. The reference result and errors in the converged P_f estimates obtained by different active learning methods are shown in Table 3. The numbers of training data required for different approaches are also provided in Table 3. Unlike in the previous examples, the ASBR-P1-MCS approach takes fewer iterations than the ASBR-P2-MCS approach. However, the accuracy of the ASBR-P2-MCS approach (the error is less than 1%) is better than that of the ASBR-P1-MCS approach (the error is greater than 5%). On the other hand, the convergence of the AK-MCS method is attained for $\varepsilon_{thr} = 5\%$ after a large number of iterations (12 + 596 training data). Though the error threshold is taken at 5%, the true error is found to be less

than 1%. It is realized that considering the 1% error threshold only increases the number of iterations without significantly improving the estimates of the P_f values. Therefore, the ESC-based AK-MCS method is not performed for $\varepsilon_{thr} = 1\%$. The error of the proposed ASBR-P2-MCS approach to estimate the P_f value is less than 1% with 211 iterations, i.e., requires a total of 222 (12 + 210) numbers of training data. Hence, the efficiency of the proposed ASBR-P2-MCS approach is also superior for this high-dimensional problem. To study the performance of the present algorithm for the estimation of smaller probabilities, the P_f values are further obtained by relaxing the value of u_0 to 0.0568. The reliability results obtained by different approaches are shown in Table 3. A similar observation is also noted for this smaller failure probability case.

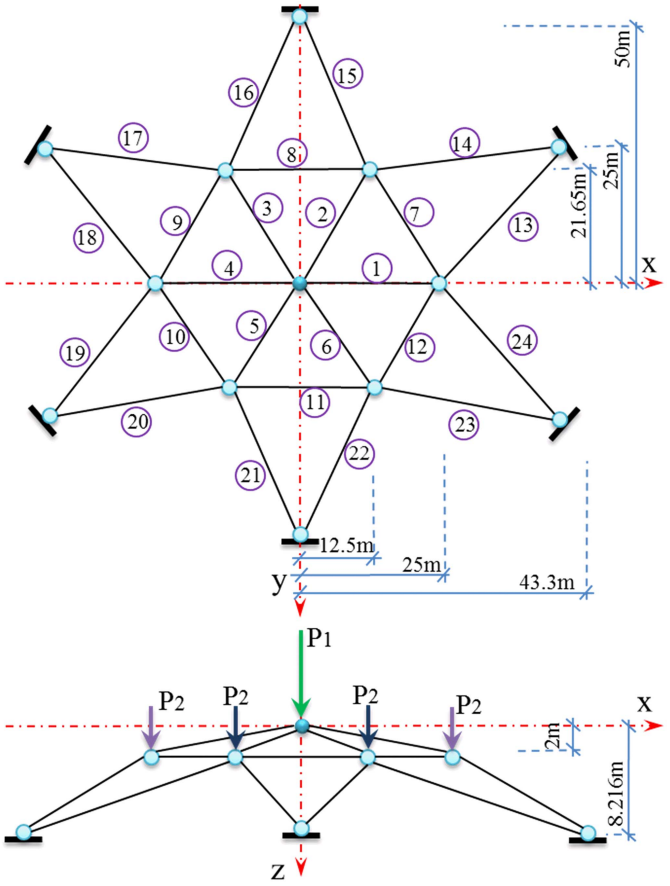

Fig. 6. Schematic diagram of the space-dome truss. (Reprinted from *Applied Mathematical Modelling*, Vol. 45, B. Keshtegar, "A hybrid conjugate finite-step length method for robust and efficient reliability analysis," pp. 226–237, © 2017, with permission from Elsevier.)

The convergences of the P_f values at each iteration by different active learning methods are shown in Fig. 8. Unlike the previous problems, the P_f values estimated by the AK-MCS algorithm reach the proximity of the actual value slower than the proposed ASBR-MCS approaches. This indicates the advantage of applying sparse Bayesian regression instead of the Kriging metamodel for a high-dimensional problem.

Further, the performances of different approaches are studied for varying dimensions of the problem. The values of P_f for $u_0 = 0.0056$ are obtained by the brute-force MCS technique as 0.01379, 0.01385, 0.0139, and 0.01397 for $N = 45$, 50, 55, and 60, respectively. The numbers of training data required and absolute errors in estimating the P_f values by the proposed approaches (ASBR-P1-MCS and ASBR-P2-MCS) and AK-P0-MCS method for $\varepsilon_{thr} = 5\%$ are compared in Fig. 9. In all cases, AK-P0-MCS for $\varepsilon_{thr} = 5\%$ takes a larger number of samples. The accuracy of ASBR-P2-MCS and AK-P0-MCS for $\varepsilon_{thr} = 5\%$ are comparable (less than 1%, i.e., practically negligible). This shows the effectiveness of the proposed ASBR-P2-MCS approach for varying dimensions.

Example 4: High-Dimensional Benchmark Problem

Another benchmark problem (a flexible dimension problem) originally proposed by Rackwitz (2001) is studied for further numerical elucidation. This example was also studied by Echard et al. (2011) and others (Huang et al. 2016; Wang and Shafieezadeh 2019) for active learning-based reliability analysis. The LSF is defined as

$$g = n + 3\sqrt{\sigma} - \sum_{i=1}^{N} x_i \tag{22}$$

Table 2. Results of different reliability methods for the space-dome truss

Reliability method	Stopping criteria for learning	P_f for Δ_{allow} = 0.01 m	0.0105 m	0.011 m	0.0115 m
MCS	—	3.353×10^{-2}	1.915×10^{-2}	1.044×10^{-2}	5.75×10^{-3}
		P_f, absolute error, number of data [lower and upper bounds of confidence interval]			
AK-P0-MCS	ESC, $\varepsilon_{thr} = 5\%$	3.446×10^{-2}, 2.77%, 12 + 7 [3.3×10^{-2}, 3.599×10^{-2}]	1.961×10^{-2}, 2.40%, 12 + 8 [1.87×10^{-2}, 2.064×10^{-2}]	1.043×10^{-2}, 0.10%, 12 + 12 [0.997×10^{-2}, 1.091×10^{-2}]	5.62×10^{-3}, 2.26%, 12 + 17 [5.39×10^{-3}, 5.869×10^{-3}]
	ESC, $\varepsilon_{thr} = 1\%$	3.355×10^{-2}, 0.06%, 12 + 33 [3.327×10^{-2}, 3.387×10^{-2}]	1.937×10^{-2}, 1.15%, 12 + 37 [1.918×10^{-2}, 1.955×10^{-2}]	1.04×10^{-2}, 0.38%, 12 + 37 [1.031×10^{-2}, 1.049×10^{-2}]	5.78×10^{-3}, 0.52%, 12 + 43 [5.73×10^{-3}, 5.825×10^{-3}]
ASBR-P1-MCS	Maxdev10 < 1%	3.238×10^{-2}, 3.43%, 12 + 47 [2.941×10^{-2}, 3.609×10^{-2}]	1.918×10^{-2}, 0.16%, 12 + 31 [1.703×10^{-2}, 2.198×10^{-2}]	1.047×10^{-2}, 0.29%, 12 + 39 [0.891×10^{-2}, 1.260×10^{-2}]	5.57×10^{-3}, 3.13%, 12 + 58 [4.74×10^{-3}, 6.68×10^{-3}]
ASBR-P2-MCS	Maxdev10 < 1%	3.352×10^{-2}, 0.03%, 12 + 31 [3.289×10^{-2}, 3.415×10^{-2}]	1.923×10^{-2}, 0.42%, 12 + 24 [1.9×10^{-2}, 1.938×10^{-2}]	1.034×10^{-2}, 0.96%, 12 + 30 [1.018×10^{-2}, 1.047×10^{-2}]	5.83×10^{-3}, 1.39%, 12 + 28 [5.71×10^{-3}, 5.92×10^{-3}]

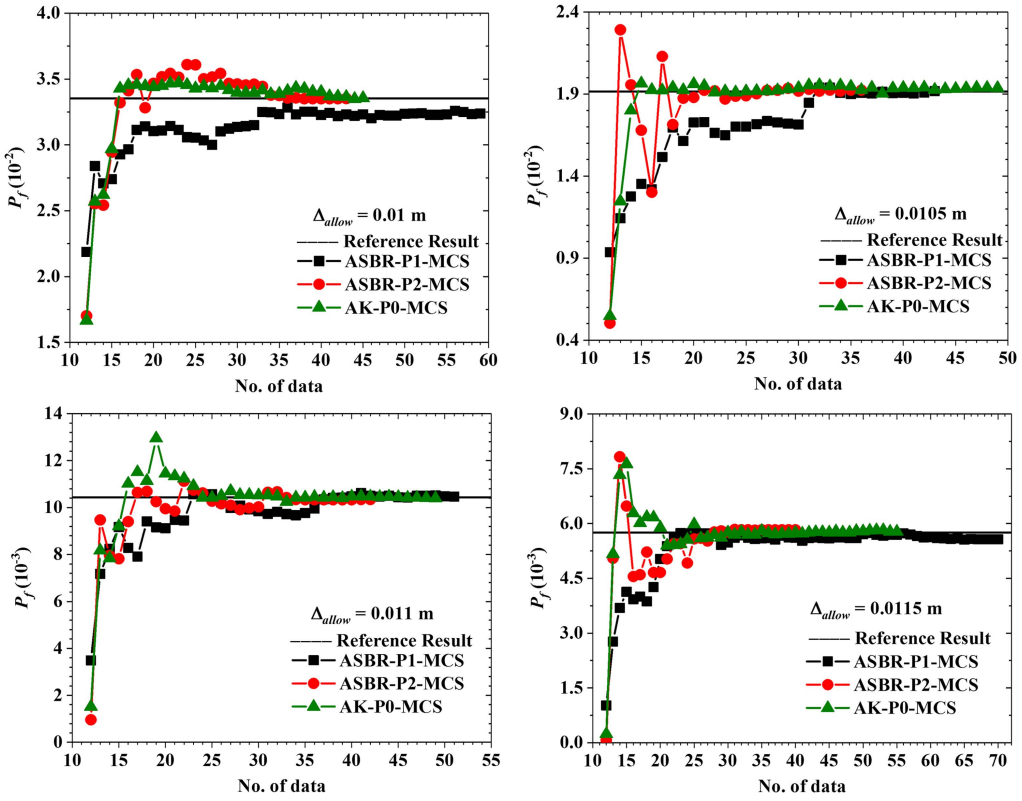

Fig. 7. Comparison of the results obtained by different active learning reliability methods for the space-dome truss.

Table 3. Results of different reliability methods for the heat conduction problem considering 75 dimensions

Reliability method	Stopping criteria for learning	P_f for u_0 = 0.0056	P_f for u_0 = 0.00568
MCS	—	1.424×10^{-2}	5.08×10^{-3}
		P_f, absolute error, number of data [lower and upper bounds of confidence interval]	
AK-P0-MCS	ESC, $\varepsilon_{thr} = 5\%$	1.422×10^{-2}, 0.14%, 12 + 596 [1.374×10^{-2}, 1.497×10^{-2}]	5.09×10^{-3}, 0.20%, 12 + 515 [4.98×10^{-3}, 5.354×10^{-3}]
ASBR-P1-MCS	Maxdev10 < 1%	1.342×10^{-2}, 5.76%, 12 + 63 [1.244×10^{-2}, 1.467×10^{-2}]	5×10^{-3}, 1.57%, 12 + 108 [4.45×10^{-3}, 5.701×10^{-3}]
ASBR-P2-MCS	Maxdev10 < 1%	1.431×10^{-2}, 0.49%, 12 + 210 [1.426×10^{-2}, 1.436×10^{-2}]	5.1×10^{-3}, 0.39%, 12 + 264 [5.07×10^{-3}, 5.13×10^{-3}]

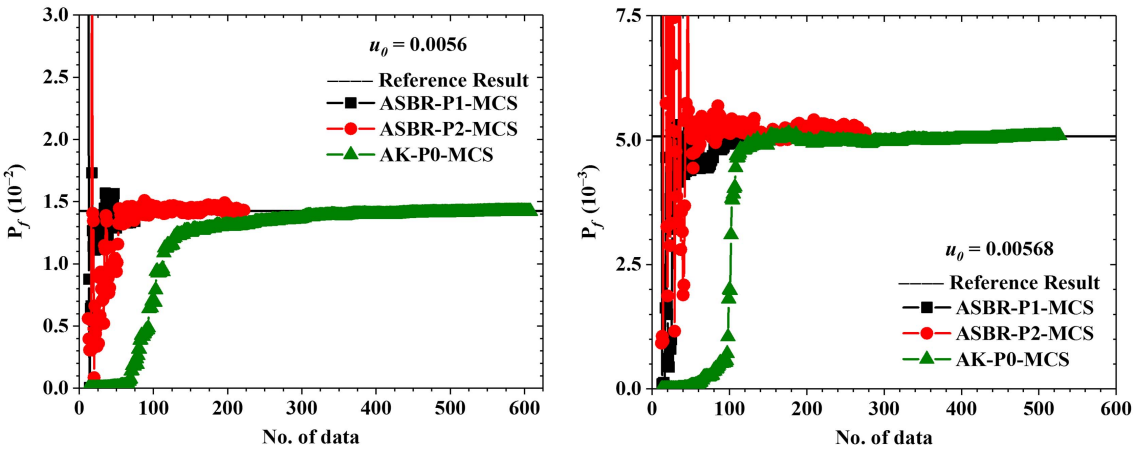

Fig. 8. Comparison of the results obtained by different active learning reliability methods for the heat conduction problem considering 75 dimensions.

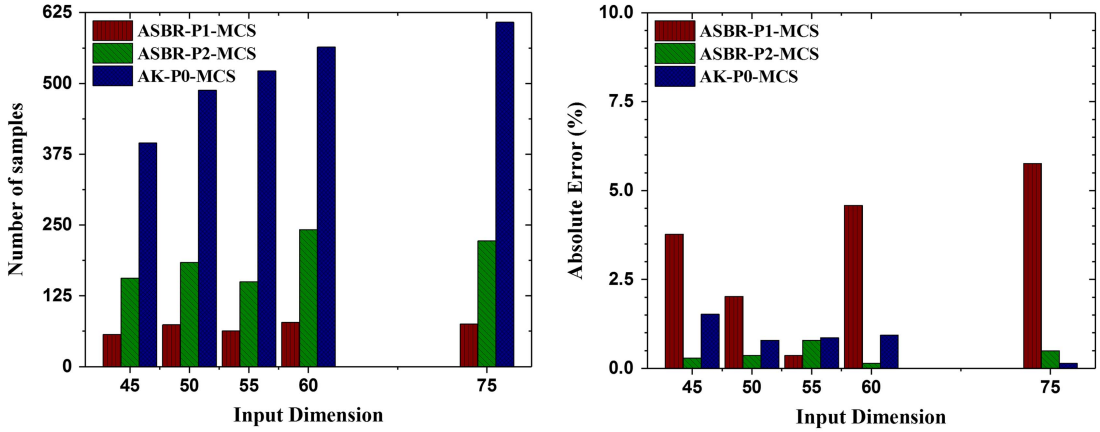

Fig. 9. Comparison of efficiency and accuracy of different active learning reliability methods for the heat conduction problem with varying dimensions.

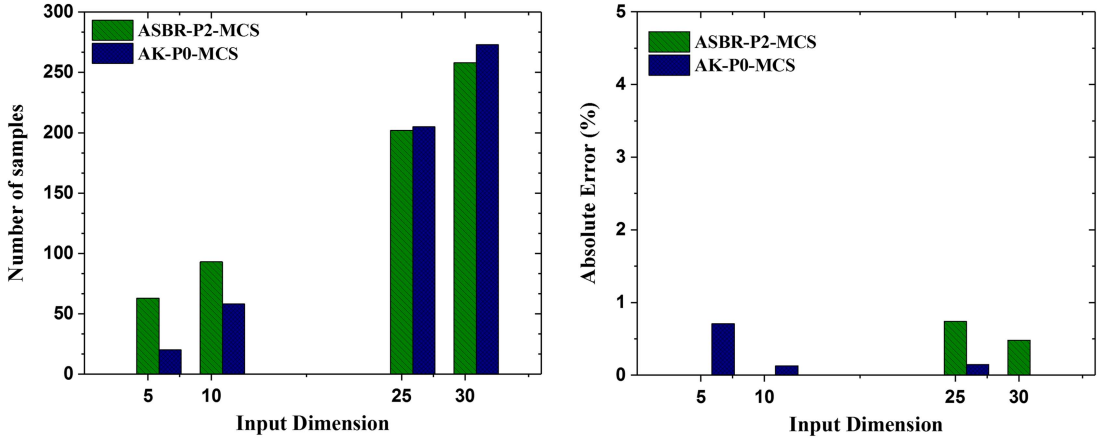

Fig. 10. Comparison of efficiency and accuracy of different active learning reliability methods for the high-dimensional benchmark problem with varying dimensions.

where N = the number of input dimensions, and all the input variables follow a lognormal distribution with unit mean and SD, $\sigma = 0.2$. In the present study, the P_f values are obtained by two active learning approaches (ASBR-P2-MCS and AK-P0-MCS for $\varepsilon_{thr} = 5\%$) for $N = 5$, 10, 25, and 30. The reference results based on the brute-force MCS technique using 3×10^5 samples are 3.3×10^{-3}, 2.603×10^{-3}, 2.257×10^{-3}, and 2.077×10^{-3} for $N = 5$, 10, 25, and 30, respectively. The number of training samples required and the absolute percentage error for the two active learning approaches are compared in Fig. 10. Both approaches estimate the P_f values with good accuracy (errors less than 1%). It may be noted that, although the ASBR-P2-MCS takes a larger number of samples than AK-P0-MCS for $N = 5$ and 10, fewer samples are required by ASBR-P2-MCS than AK-P0-MCS for higher dimensions, i.e., $N = 25$ and 30.

Example 5: Multistoried Building Frame under Earthquake Loading

The last example is a more realistic four-story building frame subjected to earthquake loading. The same building frame was studied earlier by Ghosh et al. (2018) for seismic reliability analysis. The building frame is 13.5 m high, having beams of 0.3 m width and 0.4 m depth, reinforced with three 16 mm diameter bars provided longitudinally at the top and bottom. The stirrups of 8 mm diameter are provided at a spacing of 0.2 m. The square columns of 0.4 m × 0.4 m cross-sections are reinforced with 12 16 mm diameter bars equally placed longitudinally, and lateral ties of 8 mm diameter are provided at a spacing of 0.2 m. The nonlinear time history analysis of the frame is performed in the OpenSees software. The building plan, details of the selected frame, and the FE modeling of the frame with associated fiber discretization of the beams and columns can be found in Ghosh et al. (2018). The applied ground motion is taken from the elcentro_NS.dat file available at http://www.vibrationdata.com/elcentro.htm. The characteristic strength of concrete (f_{ck}), yield strength of reinforcing steel (f_y), and structural damping ratio (ξ) are considered random variables. The random variables are assumed to be correlated truncated normal with mean values of 25 MPa, 250 MPa, and 5%; the truncation limits are [20,30] MPa, [200,300] MPa, and [3,7] % for f_{ck}, f_y, and ξ, respectively. The COVs of f_{ck} and f_y are 0.2 and that of ξ is 0.4. The coefficient of correlation between f_{ck} and ξ is taken as 0.2 and that between f_y and ξ is taken as 0.1.

The reliability is obtained for the maximum lateral displacement of the frame not exceeding a threshold value. The threshold of maximum lateral displacement is taken as 0.28 m. The reference result is obtained by the brute-force MCS technique using 10^5 samples. The P_f values, absolute errors, numbers of training data required, and

Table 4. Results of different reliability methods for the building frame

Reliability method	Stopping criteria for learning	P_f for maximum allowable total drift = 0.28 m
MCS	—	3.272×10^{-2}
		P_f, absolute error, number of data [lower and upper bounds of confidence interval]
AK-P0-MCS	ESC, $\varepsilon_{thr} = 5\%$	2.941×10^{-2}, 10.12%, 12 + 1,202 [2.835×10^{-2}, 3.072×10^{-2}]
ASBR-P1-MCS	Maxdev10 < 1%	2.304×10^{-2}, 29.58%, 12 + 61 [1.756×10^{-2}, 3.228×10^{-2}]
ASBR-P2-MCS	Maxdev10 < 1%	3.064×10^{-2}, 6.36%, 12 + 54 [2.487×10^{-2}, 3.940×10^{-2}]

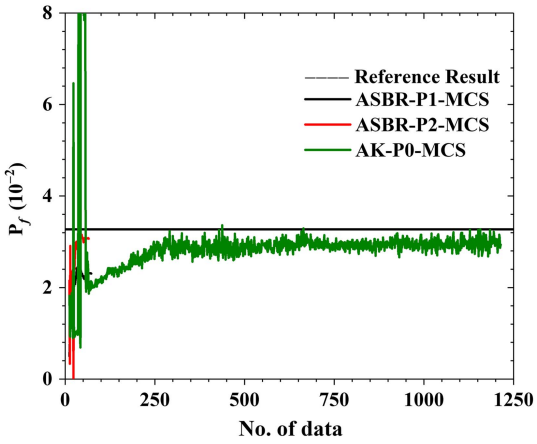

Fig. 11. Comparison of the results obtained by different active learning reliability methods for the building frame.

the lower and upper bounds of the P_f values obtained by the AK-P0-MCS (for $\varepsilon_{thr} = 5\%$), the proposed ASBR-P1-MCS and ASBR-P2-MCS approaches are shown in Table 4. The ASBR-P2-MCS is found to be the most accurate, requiring the least number of samples (12 + 54), which indicates the effectiveness of the proposed ASBR-P2-MCS. On the other hand, the AK-P0-MCS method for $\varepsilon_{thr} = 5\%$ takes a large number of samples (i.e., 12 + 1,202). Thus, the AK-P0-MCS method for $\varepsilon_{thr} = 1\%$ is not attempted apprehending that it will take much more samples for convergence. The convergences for the estimation of the P_f values at each iteration by different active learning methods are compared in Fig. 11. As with Example 3, the P_f value estimated by the AK-MCS method reaches the proximity of the actual value much slower than the proposed ASBR-MCS approaches. This also shows the advantage of reliability estimate by the sparse Bayesian regression over the Kriging metamodel for this realistic problem.

Summary and Conclusion

Active learning-enhanced adaptive sampling-based sparse Bayesian regression with first- and second-order polynomial basis functions is studied for reliability analysis. The polynomial basis functions employed here do not involve free parameters. Thus, the approach avoids expensive parameter tuning. The performance of the proposed ASBR-MCS approach is compared with the ESC-based AK-MCS method for five numerical problems over a wide range of parameters. The overall performance of the ASBR-P2-MCS approach is observed to be better than the ASBR-P1-MCS approach. Thereby, the ASBR-P2-MCS approach is more appropriate for reliability estimation problems involving implicit LSF. The accuracy level of the proposed ASBR-P2-MCS approach is comparable with the ESC-based AK-MCS method. Also, the training data required by these two approaches are found to be similar for the first two examples. However, the proposed ASBR-P2-MCS approach requires much less training data than the ESC-based AK-MCS method for high dimensional cases, as noted in the third and fourth examples. The present ASBR-P2-MCS approach is observed to be more efficient than the ESC-based AK-MCS method in terms of sample requirement and accuracy for the more realistic multistoried building frame reliability analysis problem involving nonlinear dynamic analysis. The proposed adaptive sparse Bayesian regression algorithm is generic in nature and can be integrated further with advanced MCS techniques for estimating small failure probability. The performance of the proposed ASBR-MCS approach for reliability analysis involving multiple LSFs requires further study.

Data Availability Statement

All data, models, or code that support the findings of this study are available from the corresponding author upon reasonable request.

References

Bichon, B. J., M. S. Eldred, L. P. Swiler, S. Mahadevan, and J. M. McFarland. 2008. "Efficient global reliability analysis for nonlinear implicit performance functions." *AIAA J.* 46 (10): 2459–2468. https://doi.org/10.2514/1.34321.

Blatman, G., and B. Sudret. 2010. "An adaptive algorithm to build up sparse polynomial chaos expansions for stochastic finite element analysis." *Probab. Eng. Mech.* 25 (2): 183–197. https://doi.org/10.1016/j.probengmech.2009.10.003.

Changcong, Z., L. Zhenzhou, Z. Feng, and Y. Zhufeng. 2015. "An adaptive reliability method combining relevance vector machine and importance sampling." *Struct. Multidiscip. Optim.* 52 (5): 945–957. https://doi.org/10.1007/s00158-015-1287-z.

Cheng, K., and Z. Lu. 2021. "Adaptive Bayesian support vector regression model for structural reliability analysis." *Reliab. Eng. Syst. Saf.* 206 (Feb): 107286. https://doi.org/10.1016/j.ress.2020.107286.

Choi, S.-K., R. V. Grandhi, and R. A. Canfield. 2007. *Reliability-based structural design*. London: Springer-Verlag.

Deng, J. 2006. "Structural reliability analysis for implicit performance function using radial basis function network." *Int. J. Solids Struct.* 43 (11–12): 3255–3291. https://doi.org/10.1016/j.ijsolstr.2005.05.055.

Ditlevsen, O., and H. O. Madsen. 2005. *Structural reliability methods*. Chichester, UK: Wiley.

Dubourg, V., B. Sudret, and J. M. Bourinet. 2011. "Reliability-based design optimization using kriging surrogates and subset simulation." *Struct. Multidiscip. Optim.* 44 (5): 673–690. https://doi.org/10.1007/s00158-011-0653-8.

Echard, B., N. Gayton, and M. Lemaire. 2011. "AK-MCS: An active learning reliability method combining Kriging and Monte Carlo Simulation." *Struct. Saf.* 33 (2): 145–154. https://doi.org/10.1016/j.strusafe.2011.01.002.

Echard, B., N. Gayton, M. Lemaire, and N. Relun. 2013. "A combined importance sampling and Kriging reliability method for small failure probabilities with time-demanding numerical models." *Reliab. Eng. Syst. Saf.* 111 (Mar): 232–240. https://doi.org/10.1016/j.ress.2012.10.008.

Faravelli, L. 1989. "Response-surface approach for reliability analysis." *J. Eng. Mech.* 115 (12): 2763–2781. https://doi.org/10.1061/(ASCE)0733-9399(1989)115:12(2763).

Ghosh, S., A. Roy, and S. Chakraborty. 2018. "Support vector regression based metamodeling for seismic reliability analysis of structures." *Appl. Math. Modell.* 64 (Dec): 584–602. https://doi.org/10.1016/j.apm.2018.07.054.

Haldar, A., and S. Mahadevan. 2000. *Probability, reliability, and statistical methods in engineering design*. New York: Wiley.

Hosni Elhewy, A., E. Mesbahi, and Y. Pu. 2006. "Reliability analysis of structures using neural network method." *Probab. Eng. Mech.* 21 (1): 44–53. https://doi.org/10.1016/j.probengmech.2005.07.002.

Huang, X., J. Chen, and H. Zhu. 2016. "Assessing small failure probabilities by AK-SS: An active learning method combining Kriging and subset simulation." *Struct. Saf.* 59 (Mar): 86–95. https://doi.org/10.1016/j.strusafe.2015.12.003.

Kaymaz, I. 2005. "Application of kriging method to structural reliability problems." *Struct. Saf.* 27 (2): 133–151. https://doi.org/10.1016/j.strusafe.2004.09.001.

Keshtegar, B. 2017. "A hybrid conjugate finite-step length method for robust and efficient reliability analysis." *Appl. Math. Modell.* 45 (May): 226–237. https://doi.org/10.1016/j.apm.2016.12.027.

Kim, C., S. Wang, and K. K. Choi. 2005. "Efficient response surface modeling by using moving least-squares method and sensitivity." *AIAA J.* 43 (11): 2404–2411. https://doi.org/10.2514/1.12366.

Lagaros, N. D., Y. Tsompanakis, P. N. Psarropoulos, and E. C. Georgopoulos. 2009. "Computationally efficient seismic fragility analysis of geostructures." *Comput. Struct.* 87 (19–20): 1195–1203. https://doi.org/10.1016/j.compstruc.2008.12.001.

Li, H. S., Z. Lü, Z. F. Yue, Z. Z. Lu, and Z. F. Yue. 2006. "Support vector machine for structural reliability analysis." *Appl. Math. Mech.* 27 (10): 1295–1303. https://doi.org/10.1007/s10483-006-1001-z.

Li, T. Z., Q. Pan, and D. Dias. 2021. "Active learning relevant vector machine for reliability analysis." *Appl. Math. Modell.* 89 (Jan): 381–399. https://doi.org/10.1016/j.apm.2020.07.034.

Marelli, S., and B. Sudret. 2018. "An active-learning algorithm that combines sparse polynomial chaos expansions and bootstrap for structural reliability analysis." *Struct. Saf.* 75 (Nov): 67–74. https://doi.org/10.1016/j.strusafe.2018.06.003.

Mathur, S., and P. Samui. 2013. "Application of relevance vector machine for structural reliability analysis." In *Proc., of Int. Conf. on Advances in Civil Engineering*, 961–967. New Delhi, India: Indian Society of Technical Education.

Metya, S., T. Mukhopadhyay, S. Adhikari, and G. Bhattacharya. 2017. "System reliability analysis of soil slopes with general slip surfaces using multivariate adaptive regression splines." *Comput. Geotech.* 87 (Jul): 212–228. https://doi.org/10.1016/j.compgeo.2017.02.017.

Rackwitz, R. 2001. "Reliability analysis-a review and some perspective." *Struct. Saf.* 23 (4): 365–395. https://doi.org/10.1016/S0167-4730(02)00009-7.

Roy, A., and S. Chakraborty. 2020. "Support vector regression based metamodel by sequential adaptive sampling for reliability analysis of structures." *Reliab. Eng. Syst. Saf.* 200 (Aug): 106948. https://doi.org/10.1016/j.ress.2020.106948.

Roy, A., R. Manna, and S. Chakraborty. 2019. "Support vector regression based metamodeling for structural reliability analysis." *Probab. Eng. Mech.* 55 (Jan): 78–89. https://doi.org/10.1016/j.probengmech.2018.11.001.

Schöbi, R., B. Sudret, and S. Marelli. 2017. "Rare event estimation using polynomial-chaos kriging." *ASCE-ASME J. Risk Uncertainty Eng. Syst. Part A: Civ. Eng.* 3 (2): D4016002. https://doi.org/10.1061/AJRUA6.0000870.

Tipping, M. E. 2001. "Sparse Bayesian learning and the relevance vector machine." *J. Mach. Learn. Res.* 1 (3): 211–244.

Tipping, M. E., and A. C. Faul. 2003. "Fast marginal likelihood maximisation for sparse bayesian models hyper-spectral classification view project fast marginal likelihood maximisation for sparse bayesian models." In *Proc., 9th Int. Workshop on Artificial Intelligence and Statistics*, edited by B. J. Bishop and C. M. Frey. Key West, FL: Society for Artificial Intelligence and Statistics.

Wang, Z., and A. Shafieezadeh. 2019. "ESC: An efficient error-based stopping criterion for kriging-based reliability analysis methods." *Struct. Multidiscip. Optim.* 59 (5): 1621–1637. https://doi.org/10.1007/s00158-018-2150-9.

Xu, C., W. Chen, J. Ma, Y. Shi, and S. Lu. 2020. "AK-MSS: An adaptation of the AK-MCS method for small failure probabilities." *Struct. Saf.* 86 (Sep): 101971. https://doi.org/10.1016/j.strusafe.2020.101971.

Zhang, X., L. Wang, and J. D. Sørensen. 2020. "AKOIS: An adaptive Kriging oriented importance sampling method for structural system reliability analysis." *Struct. Saf.* 82 (Jan): 101876. https://doi.org/10.1016/j.strusafe.2019.101876.

Zhou, C., Z. Lu, and X. Yuan. 2013. "Use of relevance vector machine in structural reliability analysis." *J. Aircr.* 50 (6): 1726–1733. https://doi.org/10.2514/1.C031950.

Zhou, Y., Z. Lu, and W. Yun. 2020. "Active sparse polynomial chaos expansion for system reliability analysis." *Reliab. Eng. Syst. Saf.* 202 (Oct): 107025. https://doi.org/10.1016/j.ress.2020.107025.